Effects of shell structure and N/Z ratio of a projectile on the excitation energy distribution between interacting nuclei in deep-inelastic collisions

G. G. Adamian,* R. V. Jolos, and A. K. Nasirov*
Joint Institute for Nuclear Research, 141980 Dubna, Russia

A. I. Muminov
Heavy Ion Physics Department, Institute of Nuclear Physics, 702132 Ulugbek, Uzbekistan
(Received 13 April 1995)

Deep inelastic collisions of stable and radioactive projectiles with heavy targets are considered. The effects of shell structure and the N/Z ratio of a projectile on the excitation energy distribution between interacting nuclei, and on the centroid position and variance of the charge (mass) distribution of binary reaction products are explored. The role of nucleon exchange and particle-hole excitation mechanisms in the transformation of relative motion kinetic energy into the internal excitation energy of nuclei is studied. It is shown that a change in the mass number of the projectile nucleus causes a sufficient change both in the sharing of the excitation energy between fragments and in the charge (mass) distribution of reaction products. The nucleon exchange process between interacting nuclei is the main mechanism of dissipation.

PACS number(s): 25.70.Hi, 25.70.Lm

I. INTRODUCTION

A large value for kinetic energy losses is an inherent feature of deep inelastic heavy ion collisions [1,2]. Earlier it was assumed that the relative motion kinetic energy of nuclei, being transformed into intrinsic excitation energy, was distributed between reaction products in approximate proportion to their masses. Recent experiments [3–14], however, have demonstrated that this assumption is incorrect. For example, in the ^{58}Ni+^{197}Au [3,4], ^{56}Fe,^{74}Ge + ^{165}Ho reactions [5–12] the excitation energy is about equally divided between the products of the binary reactions for relatively large values of the total kinetic energy losses. In other reactions [3,13,14], the excitation energy distribution is intermediate between equal sharing and sharing proportionate to the fragment masses. In the ^{52}Cr+^{208}Pb [13], ^{238}U+^{124}Sn, ^{110}Pd reactions [14] a large part of the excitation energy is concentrated in the light fragments even for a wide range of total kinetic energy loss. These new experiments created a great interest in the problem of kinetic energy dissipation. To reconstruct the primary reaction product yields from the measured evaporation residues, it is important to know how the excitation energy was distributed between the primary fragments.

The fact that thermodynamic equilibrium is not attained as quickly as it was assumed earlier points to the important role of the structure of interacting nuclei even at relatively large kinetic energy losses. The effect of shell structure on the energy dissipation is manifested in the experimental study of the correlation of the total kinetic energy loss with the nucleon exchange between interacting nuclei [2–12,15,16]. The value of the total kinetic energy loss per unit of the charge distribution variance of the products for the ^{208}Pb + ^{208}Pb reaction is significantly larger than that for the ^{238}U + ^{238}U reaction [15,16]. The effect of the neutron number variation of the projectile nucleus on the mass, charge, and energy distributions of deep inelastic heavy ion collision products is studied in [17–23].

Interesting results for the yields of neutron-rich nuclei in the incomplete fusion reactions of ^{40,44,48}Ca + ^{248}Cm were obtained in [18,20]. The observed yields of such elements as Th, U, and Pu in the reaction with ^{40}Ca turned out to be two orders of magnitude smaller than those in the reaction with ^{48}Ca. The cross section of production for elements with masses larger than the target-nucleus mass, however, is of two orders of magnitude larger for the reaction with ^{44}Ca than that for the reaction with ^{48}Ca. From analysis of the N/Z ratio (N and Z are the neutron and proton numbers) of distribution of secondary nuclides the authors concluded that targetlike fragments have small excitation energies. This fact should be taken into account in deexcitation calculations [23]. The difference in excitation energy values in all three ^{40,44,48}Ca + ^{248}Cm reactions is assumed to be related to the difference in Q_{gg} values.

The effect of the shell structure and N/Z ratio of the projectile on the partitioning of excitation energy between interacting nuclei, as well as on mass and charge distributions of the products of deep inelastic heavy ion collisions, is studied in [18,20]. It is evident that the analysis of this effect should be based on a microscopic model.

The calculation of frictional coefficients requires explicit formulation of a microscopical model, including the coupling of relative motion to the intrinsic degrees of freedom [24–41]. These models are distinguished by the intrinsic excitations to be considered: collective surface vibrations, giant resonances, noncoherent particle-hole excitations, or nucleon exchange between nuclei. It is clear that the structure of excited states and the strength of the coupling of different excitation modes with a relative motion will affect the excitation energy distribution between fragments.

*On leave from Heavy Ion Physics Department, Institute of Nuclear Physics, 702132 Ulugbek, Tashkent, Uzbekistan.

The most commonly used models are those based on the one-body dissipation approach [29,40]. In these models, the friction force is determined by the nucleon exchange through a ''window'' during nuclear collision [42]. The simplicity of this model [29,40] and its success in describing the kinetic energy loss and the width of the mass (charge) distribution of reaction products are encouraging. The interacting nuclei in the framework of these models, however, are considered in the Fermi-gas approximation, and therefore, the nuclear structure is taken into account only by means of averaging over the ground state energy and parameters of the level density.

One of the advantages of our model [43,44] as compared with model [29,40] is that it allows us to explicitly take into account the effect of the nuclear shell structure on a collision process. A realistic scheme of single-particle states, nucleon separation energies, and single-particle matrix elements of nucleon transitions both in each nucleus and from one nucleus to another are constituents of our model. The single-particle approach is improved by the phenomenological account of the residual interaction between nucleons. Experimental data on the widths and centroid positions of the charge (mass) distributions of the reaction products indicate that as dinuclear systems evolve individual features of the nuclei are preserved, and shell structure effects play an important part [1,2]. In comparison with model [29,40] our model gives correct direction of proton and neutron drifts. It is known that the nucleon drift also renders the influence on the process of excitation energy division between fragments [3]. Another advantage of our model is the possibility of simultaneously considering the particle-hole excitations in each nucleus and the nucleon exchange between nuclei. The particle-hole excitation mechanism seems to be an essential contribution at peripheral internuclear distances. This excitations become as important as a nucleon exchange especially for the massive dinuclear systems [43]. In the framework of this model, a good agreement with the experimental results has been obtained in describing the dependence of the excitation energy sharing between reaction products on their mass number, and the dependence of the centroid position and variances of the charge and mass distributions on the total kinetic energy loss [43,44].

The basic features of our model are described in Sec. II. In Sec. III, the effects of the projectile shell structure and its N/Z ratio on excitation energy distribution, centroid position, and variance of the charge (mass) distribution for binary reaction products in deep inelastic heavy ion collisions are explored. The role of nucleon exchange and particle-hole excitation mechanisms in the transformation of relative motion kinetic energy into the internal excitation energy of nuclei is studied. Conclusions are given in Sec. IV.

II. MODEL

The model is based on the assumption that colliding nuclei moving along approximately classical trajectories preserve most of their individual properties during the interaction time at the kinetic energies under consideration [1,2,45]. For this reason, the quantum-mechanical consideration of the intrinsic degrees of freedom employs the single-particle approximation with a realistic scheme of the single-particle levels for each nucleus. Each nucleus is described by a potential well (Woods-Saxon-type potential) with nucleons in it. The interaction picture can be represented as follows: During the interaction time both potential wells act on the nucleons of each nucleus causing nucleon transitions between single-particle states. The transitions occurring in each nucleus are particle-hole excitations, while those between partner nuclei are nucleon exchanges. Thus, in the suggested model, the single-particle mechanism is considered as the main mechanism of excitation and dissipation. The single-particle approach is improved by the phenomenological account of the residual interaction between nucleons. Such effects as excitations of high- and low-lying collective states of the interacting nuclei are neglected. Although contributions to the dissipation could come from easily excited surface vibrations, the adiabaticity of the relative motion with respect to these vibrations decreases their effects.

The total Hamiltonian of a dinuclear system $\hat{H}$ takes the form

$$\hat{H}=\hat{H}_{\rm rel}+\hat{H}_{\rm in}+\hat{V}_{\rm int}. \tag{1}$$

The Hamiltonian of a relative motion,

$$\hat{H}_{\rm rel}=\frac{\hat{\mathbf{P}}^2}{2\mu}+\hat{U}(\hat{\mathbf{R}}),$$

consists of the kinetic energy operator and a nucleus-nucleus interaction potential $\hat{U}(\hat{\mathbf{R}})$. Here $\hat{\mathbf{R}}$ is the relative distance between the centers of mass of the fragments, $\hat{\mathbf{P}}$ is the conjugate momentum, and μ is the reduced mass of the system. The last two terms in (1) describe the intrinsic motion of nuclei and the coupling between relative and intrinsic motions (for details, see [43,44]).

The single-particle Hamiltonian of the dinuclear system $\hat{\mathscr{H}}$ is

$$\hat{\mathscr{H}}(\mathbf{R}(t))=\sum_{i=1}^{A}\left(\frac{-\hbar^2}{2m}\Delta_i+\hat{U}_P(\mathbf{r}_i-\mathbf{R}(t))+\hat{U}_T(\mathbf{r}_i)\right), \tag{2}$$

where m is the nucleon mass, and $A=A_P+A_T$ is the total number of nucleons in the system. The average single-particle potentials of a projectile U_P and a target U_T involve both the nuclear and Coulomb fields.

In the second quantization form the Hamiltonian (2) can be rewritten as

$$\hat{\mathscr{H}}(\mathbf{R}(t))=\hat{\tilde{H}}_{\rm in}(\mathbf{R}(t))+\hat{V}_{\rm int}(\mathbf{R}(t)),$$

$$\hat{\tilde{H}}_{\rm in}(\mathbf{R}(t))=\sum_i \tilde{\varepsilon}_i(\mathbf{R}(t))a_i^{\dagger}a_i$$

$$=\sum_P \tilde{\varepsilon}_P(\mathbf{R}(t))a_P^{\dagger}a_P+\sum_T \tilde{\varepsilon}_T(\mathbf{R}(t))a_T^{\dagger}a_T, \tag{3}$$

$$\hat{V}_{\rm int}(\mathbf{R}(t))=\sum_{i\neq i'} V_{ii'}(\mathbf{R}(t))a_i^{\dagger}a_{i'}$$
$$=\sum_{P\neq P'} \chi^{(T)}_{PP'}(\mathbf{R}(t))a_P^{\dagger}a_{P'}$$
$$+\sum_{T\neq T'} \chi^{(P)}_{TT'}(\mathbf{R}(t))a_T^{\dagger}a_{T'}$$
$$+\sum_{T,P} g_{PT}(\mathbf{R}(t))(a_P^{\dagger}a_T+\text{H.c.}).$$

Up to the second order in the overlap integral $\langle P|T\rangle$ [46],

$$\tilde{\varepsilon}_P(\mathbf{R}(t))=\varepsilon_P+\langle P|U_T(\mathbf{r})|P\rangle,$$
$$\tilde{\varepsilon}_T(\mathbf{R}(t))=\varepsilon_T+\langle T|U_P(\mathbf{r}-\mathbf{R}(t))|T\rangle,$$
$$\chi^{(T)}_{PP'}(\mathbf{R}(t))=\langle P|U_T(\mathbf{r})|P'\rangle, \quad (4)$$
$$\chi^{(P)}_{TT'}(\mathbf{R}(t))=\langle T|U_P(\mathbf{r}-\mathbf{R}(t))|T'\rangle,$$
$$g_{PT}(\mathbf{R}(t))=\frac{1}{2}\langle P|U_P(\mathbf{r}-\mathbf{R}(t))+U_T(\mathbf{r})|T\rangle.$$

In expression (4), $\varepsilon_{P(T)}$ are the single-particle energies of nonperturbed states in the projectile (target) nucleus. These states are characterized by a set of quantum numbers $P\equiv(n_P,j_P,l_P,m_P)$ and $T\equiv(n_T,j_T,l_T,m_T)$ corresponding to the projectile (P) and target (T) nuclei, respectively. The diagonal matrix elements $\langle P|U_T|P\rangle$ ($\langle T|U_P|T\rangle$) define the shifts in single-particle energies of the projectile (target) nucleus caused by the target (projectile) mean field. The corresponding nondiagonal matrix elements $\chi^{(T)}_{PP'}$ ($\chi^{(P)}_{TT'}$) generate particle-hole transitions in the projectile (target) nucleus. The matrix elements g_{PT} correspond to the nucleon exchange between reaction partners due to the nonstationary mean field of the dinuclear system. These matrix elements were calculated in the framework of the approach proposed by us [47,48]. The contributions of noninertial recoil effects to the matrix elements are neglected since they are small [35]. The effect of the mean field of one nucleus on states of the other nucleus is taken into account in the second order of perturbation theory:

$$\tilde{\chi}^{(T)}_{PP'}(\mathbf{R}(t))=\chi^{(T)}_{PP'}(\mathbf{R}(t))+\frac{1}{\hbar}\sum_{P''}\chi^{(T)}_{PP''}(\mathbf{R}(t))\chi^{(T)}_{P''P'}(\mathbf{R}(t))$$
$$\times\left[\frac{1}{\tilde{\omega}_{P''P}(\mathbf{R}(t))}+\frac{1}{\tilde{\omega}_{P''P'}(\mathbf{R}(t))}\right], \quad (5)$$

$$\tilde{\chi}^{(P)}_{TT'}(\mathbf{R}(t))=\chi^{(P)}_{TT'}(\mathbf{R}(t))+\frac{1}{\hbar}\sum_{T''}\chi^{(P)}_{TT''}(\mathbf{R}(t))\chi^{(P)}_{T''T'}(\mathbf{R}(t))$$
$$\times\left[\frac{1}{\tilde{\omega}_{T''T}(\mathbf{R}(t))}+\frac{1}{\tilde{\omega}_{T''T'}(\mathbf{R}(t))}\right], \quad (6)$$

$$\tilde{g}_{PT}(\mathbf{R}(t))=g_{PT}(\mathbf{R}(t))+\frac{1}{\hbar}\sum_{T'}\frac{g_{PT'}(\mathbf{R}(t))\chi^{(P)}_{T'T}(\mathbf{R}(t))}{\tilde{\omega}_{T'P}(\mathbf{R}(t))}$$
$$+\frac{1}{\hbar}\sum_{P'}\frac{\chi^{(T)}_{PP'}(\mathbf{R}(t))g_{P'T}(\mathbf{R}(t))}{\tilde{\omega}_{P'T}(\mathbf{R}(t))}, \quad (7)$$

where $\tilde{\omega}_{ik}(\mathbf{R}(t))=[\tilde{\varepsilon}_i(\mathbf{R}(t))-\tilde{\varepsilon}_k(\mathbf{R}(t))]/\hbar$.

The explicit consideration of the residual interaction requires cumbersome calculations, but linearization of the two-body collision integral simplifies the consideration. In the relaxation time approximation [49] the equation of motion for the single-particle density matrix $\hat{\tilde{n}}(t)$ is

$$i\hbar\frac{\partial\hat{\tilde{n}}(t)}{\partial t}=[\hat{\mathscr{H}}(\mathbf{R}(t)),\hat{\tilde{n}}(t)]-\frac{i\hbar}{\tau}[\hat{\tilde{n}}(t)-\hat{\tilde{n}}^{\rm eq}(\mathbf{R}(t))], \quad (8)$$

where τ is the relaxation time (which will be determined later), $\hat{\tilde{n}}^{\rm eq}(\mathbf{R}(t))$ is a local quasiequilibrium density matrix at a fixed value of the collective coordinate $\mathbf{R}(t)$:

$$\tilde{n}_i^{\rm eq}(\mathbf{R}(t))=\left[1+\exp\left(\frac{\tilde{\varepsilon}_i(\mathbf{R}(t))-\lambda_K^{(\alpha)}(t)}{\Theta_K(t)}\right)\right]^{-1}, \quad (9)$$
$$\Theta_K(t)=3.46\sqrt{[E_K^{*(Z)}(t)+E_K^{*(N)}(t)]/\langle A_K(t)\rangle},$$

where $\Theta_K(t)$, $\langle A_K(t)\rangle=\langle Z_K(t)\rangle+\langle N_K(t)\rangle$, $\lambda_K^{(\alpha)}(t)$, and $E_K^{*(\alpha)}(t)$ are the effective temperature, mass number, chemical potential, and intrinsic excitation energies for the proton ($\alpha=Z$) and neutron ($\alpha=N$) subsystems of the nucleus $K(K=P,T)$, respectively.

The τ_i is calculated in the framework of the theory of quantum liquids [50,51]:

$$\frac{1}{\tau_i^{(\alpha)}}=\frac{\sqrt{2}\pi}{32\hbar\varepsilon_{F_K}^{(\alpha)}}\left[(f_K-g)^2+\frac{1}{2}(f_K+g)^2\right]$$
$$\times[(\pi\Theta_K)^2+(\tilde{\varepsilon}_i-\lambda_K^{(\alpha)})^2]\left[1+\exp\left(\frac{\lambda_K^{(\alpha)}-\tilde{\varepsilon}_i}{\Theta_K}\right)\right]^{-1}, \quad (10)$$

where

$$\varepsilon_{F_K}^{(Z)}=\varepsilon_F\left[1-\frac{2}{3}(1+2f')\frac{\langle N_K\rangle-\langle Z_K\rangle}{\langle A_K\rangle}\right],$$
$$\varepsilon_{F_K}^{(N)}=\varepsilon_F\left[1+\frac{2}{3}(1+2f')\frac{\langle N_K\rangle-\langle Z_K\rangle}{\langle A_K\rangle}\right] \quad (11)$$

are the Fermi energies of protons and neutrons ($\epsilon_F=37$ MeV). Here $f_{\rm in}=0.09$, $f'_{\rm in}=0.42$, $f_{\rm ex}=-2.59$, $f'_{\rm ex}=0.54$, $g=0.7$ are constants of the effective nucleon-nucleon interaction [51]. The finite form of the nucleus has been taken into account by the expression [51]

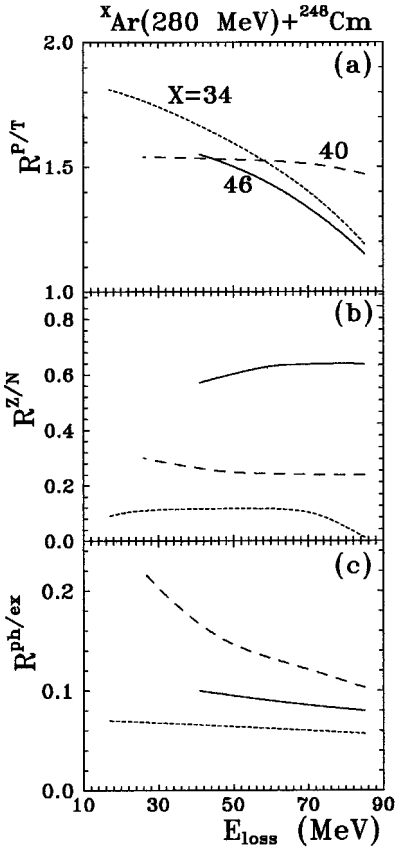

FIG. 1. The dependences of the ratios $R^{P/T}$ (a), $R^{Z/N}$ (b), and $R^{\mathrm{ph/ex}}$ (c) on E_{loss} for the $^{X}\mathrm{Ar}+^{248}\mathrm{Cm}$ reactions: $X=34$ (dotted line), $X=40$ (dashed line), $X=46$ (solid line).

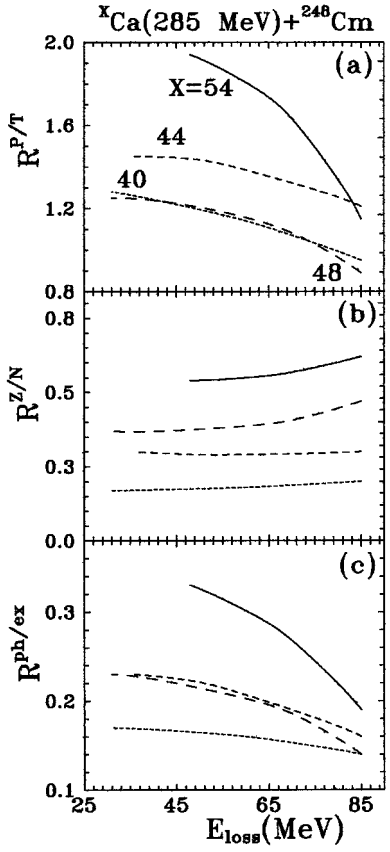

FIG. 2. The same as in Fig. 1, but for the $^{X}\mathrm{Ca}+^{248}\mathrm{Cm}$ reactions: $X=40$ (dotted line), $X=44$ (short dashed line), $X=48$ (long dashed line), $X=54$ (solid line).

$$f_K=f_{\mathrm{in}}-\frac{2}{\langle A_K\rangle^{1/3}}(f_{\mathrm{in}}-f_{\mathrm{ex}}),$$

$$f'_K=f'_{\mathrm{in}}-\frac{2}{\langle A_K\rangle^{1/3}}(f'_{\mathrm{in}}-f'_{\mathrm{ex}}). \tag{12}$$

A formal solution of Eq. (8) is

$$\tilde{n}_i(t)=\exp\left(\frac{t_0-t}{\tau_i}\right)\left\{\tilde{n}_i(t_0)+\sum_k\int_{t_0}^{t}dt'\int_{t_0}^{t'}dt''\Omega_{ik}(t',t'')\times\exp\left(\frac{t''-t}{\tau_{ik}}\right)[\tilde{n}_k(t'')-\tilde{n}_i(t'')]+\frac{1}{\tau_i}\int_{t_0}^{t}dt'\tilde{n}_i^{\mathrm{eq}}(\mathbf{R}(t'))\exp\left(\frac{t'-t_0}{\tau_i}\right)\right\}, \tag{13}$$

where

$$\Omega_{ik}(t,t')=\frac{2}{\hbar^2}\mathrm{Re}\left\{V_{ik}(\mathbf{R}(t))V_{ki}(\mathbf{R}(t'))\times\exp\left[i\int_{t'}^{t}dt''\tilde{\omega}_{ki}(\mathbf{R}(t''))\right]\right\}.$$

Equation (13) is solved step by step with the time interval $(t-t_0)$ divided into parts: t_0, $t_0+\Delta t$, $t_0+2\Delta t$, etc., for $\Delta t<\tau_i$:

$$\tilde{n}_i(t)=\tilde{n}_i^{\mathrm{eq}}(\mathbf{R}(t))\left[1-\exp\left(\frac{-\Delta t}{\tau_i}\right)\right]+n_i(t)\exp\left(\frac{-\Delta t}{\tau_i}\right), \tag{14}$$

$$n_i(t)=\tilde{n}_i(t-\Delta t)+\sum_k\overline{W}_{ik}(\mathbf{R}(t),\Delta t)\times[\tilde{n}_k(t-\Delta t)-\tilde{n}_i(t-\Delta t)], \tag{15}$$

where

$$\overline{W}_{ik}(\mathbf{R}(t),\Delta t)=|V_{ik}(\mathbf{R}(t))|^2\frac{\sin^2\left[\frac{\Delta t}{2}\tilde{\omega}_{ki}(\mathbf{R}(t))\right]}{\left[\frac{\hbar}{2}\tilde{\omega}_{ki}(\mathbf{R}(t))\right]^2}, \tag{16}$$

$n_i(t)=\langle t|a_i^{\dagger}a_i|t\rangle$ is a solution of Eq. (8) without taking into account the residual forces. The dynamic $n_i(t)$ and quasi-equilibrium $\tilde{n}_i^{(\mathrm{eq})}(\mathbf{R}(t))$ occupation numbers are calculated at every time step. The initial values of the occupation numbers equal 1 for occupied states and zero for unoccupied ones. The energy of the last complete or partially occupied level

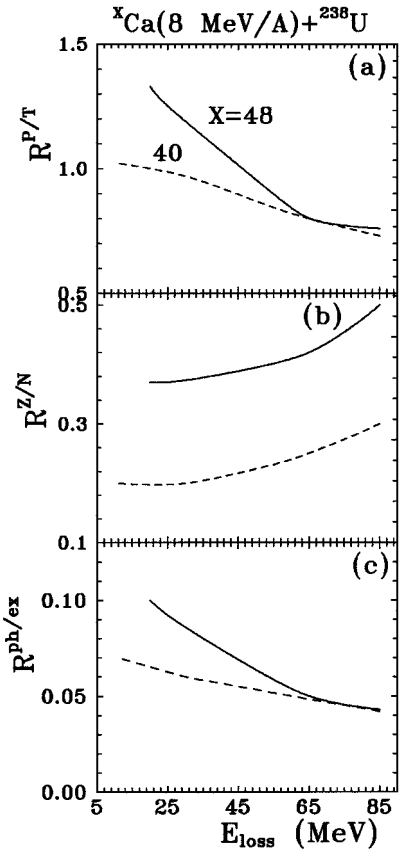

FIG. 3. The same as in Fig. 1, but for the ^{X}Ca+^{238}U reactions: $X=40$ (dashed line), $X=48$ (solid line).

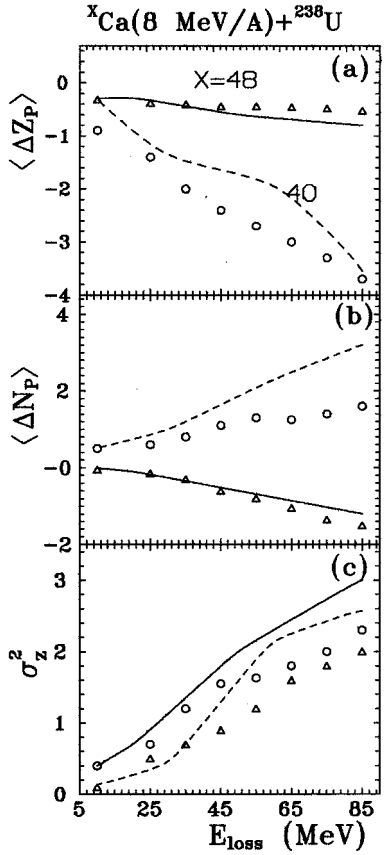

FIG. 4. The change in the mean charge $\langle \Delta Z_P \rangle$ (a) and neutron $\langle \Delta N_P \rangle$ (b) number of the projectile nucleus and the charge variance σ_Z^2 for the ^{X}Ca+^{238}U reactions as a function $E_{\rm loss}$: the dashed ($X=40$) and solid ($X=48$) lines are results of the calculations and the circles ($X=40$) and triangles ($X=48$) are the experimental data [17].

ε_i was found to be equal to the nucleon separation energy presented in [52]. The time step Δt used in the calculations is 10^{-22} s.

The present model allows us to calculate the average number of protons $\langle Z_{P(T)} \rangle$ or neutrons $\langle N_{P(T)} \rangle$, their variance σ_Z^2 or σ_N^2, and the intrinsic excitation energies $E^{*(Z)}_{P(T)}(t)$ and $E^{*(N)}_{P(T)}(t)$ for the proton and neutron subsystems of each nucleus:

$$\langle Z_{P(T)} \rangle(t) = \sum_{P(T)}^{Z} \tilde{n}_{P(T)}(t), \tag{17}$$

$$\langle N_{P(T)} \rangle(t) = \sum_{P(T)}^{N} \tilde{n}_{P(T)}(t), \tag{18}$$

$$\sigma^2_{Z(N)}(t) = \sum_{P}^{Z(N)} \tilde{n}_P(t)[1-\tilde{n}_P(t)], \tag{19}$$

$$E^{*(\alpha)}_{P(T)}(t+\Delta t) = E^{*(\alpha)}_{P(T)}(t) + \sum_{P(T)}^{(\alpha)} [\tilde{\varepsilon}_{P(T)}(\mathbf{R}(t)) - \lambda^{(\alpha)}_{P(T)}(\mathbf{R}(t))] \times [\tilde{n}_{P(T)}(t+\Delta t) - \tilde{n}_{P(T)}(t)], \tag{20}$$

where the top index $Z(N)$ of the sum restricts the summation over proton(neutron) single-particle levels. It is seen from (20) that the fragment excitation energy is calculated step by step along the time scale. Separate summing over the neutron and proton subsystems of each fragment allows us to determine their relative contribution to the excitation energy of the nuclei.

III. MODEL CALCULATIONS

This section is mainly devoted to the study of the deep inelastic heavy ion collisions of ^{34,40,46}Ar+^{248}Cm, ^{40,44,48,54}Ca+^{248}Cm, ^{40,48}Ca+^{238}U, and ^{20,22}Ne+^{248}Cm. In the framework of our model, we have analyzed the effect of the projectile N/Z ratio variations on the distribution of the excitation energy between binary products in these reactions. The shifts of the centroid position and variances of charge and mass distributions in these reactions were calculated as well. These distributions are important, for example, in choosing the combinations of reaction partners and their collision energies for synthesis of exotic nuclei. The relative motion trajectories have been calculated by the same method as in [53,54].

The following notation is used: $R^{P/T}=E^*_P/E^*_T$ is the ratio of the excitation energy of a projectilelike nucleus to a targetlike nucleus; $R^{\rm ph/ex}=E^{*(\rm ph)}/E^{*(\rm ex)}$ is the ratio of the excitation energy of nuclei produced by particle-hole excitations to that produced by nucleon exchange; $R^{Z/N}=E^{*(Z)}/E^{*(N)}$ is

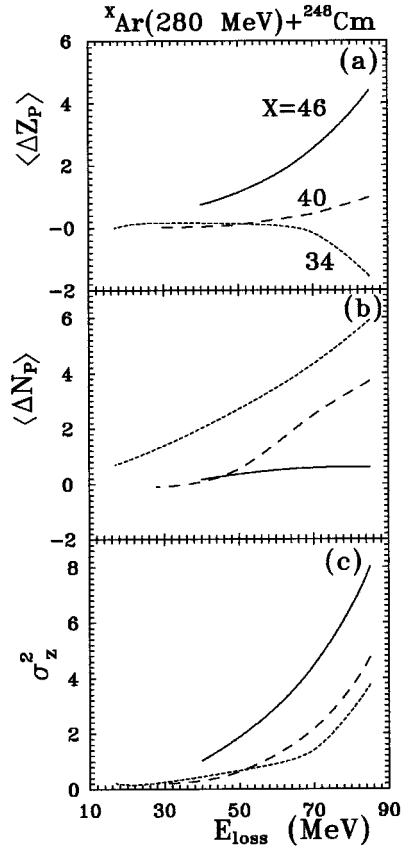

FIG. 5. The same as in Fig. 4, but for the ^{X}Ar+^{248}Cm reactions: $X=34$ (dotted line), $X=40$ (dashed line), $X=46$ (solid line).

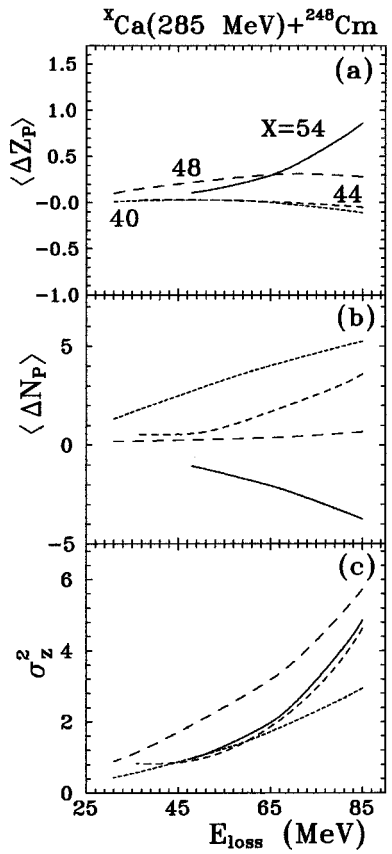

FIG. 6. The same as in Fig. 4, but for the ^{X}Ca+^{248}Cm reactions: $X=40$ (dotted line), $X=44$ (short dashed line), $X=48$ (long dashed line), $X=54$ (solid line).

the ratio of the excitation energies of the proton $E^{*(Z)}$ and neutron $E^{*(N)}$ subsystems of the dinuclear system; $\langle\Delta Z_P\rangle = Z_P - \langle Z_P\rangle$ and $\langle\Delta N_P\rangle = N_P - \langle N_P\rangle$ are the changes in the mean charge and neutron numbers in the projectile. The excitation energy of each nucleus $E_i^*(i=P,T)$ was calculated by Eq. (20) with summing of the excitation energies of the proton $E_i^{*(Z)}$ and neutron $E_i^{*(N)}$ subsystems. In all figures the abscissa presents the total excitation energy $E_{\rm loss}=E_P^*+E_T^*$.

The calculated values of $R^{P/T}$ [Figs. 1(a), 2(a), 3(a), 7(a)] show that in the ^{34,40,46}Ar+^{248}Cm, ^{40,44,48,54}Ca+ ^{248}Cm, ^{40,48}Ca+^{238}U, and ^{20,22}Ne+ ^{248}Cm reactions the excitation energy concentrated in the light products is significantly larger than that corresponding to thermodynamic equilibrium. This is seen most clearly in the results of calculations for the reactions with ^{34}Ar and ^{54}Ca. Thus, due to the short interaction time and the strong difference in the shell structures of the colliding nuclei, a thermodynamic equilibrium in the dinuclear system is not reached.

These results show that the N/Z ratio of the projectile strongly affects the excitation energy sharing between fragments. The deviation of the curve, which describes a dependence of ratio $R^{P/T}$ on $E_{\rm loss}$ in Fig. 2(a), for ^{48}Ca from the trend of other isotopes with increasing N/Z ratio manifests an important role of the nucleus shell structure into a partition of excitation between binary products of the reaction. From our calculations, it is seen [Fig. 2(a)] that the excitation energies of ^{40}Ca and ^{48}Ca are smaller as compared with ^{44}Ca and ^{54}Ca in the ^{X}Ca + ^{248}Cm reactions. The neutron level $f_{7/2}$ is filled with increasing N/Z ratio from 1 for ^{40}Ca to 1.4 for ^{48}Ca. The ratio $R^{P/T}$ increases with filling of this level [see the ^{X}Ca + ^{248}Cm reaction in Fig. 2(a)]. However, $R^{P/T}$ decreases for reaction with magic nucleus ^{48}Ca, for which level $f_{7/2}$ is completely occupied. As for isotopes heavier than ^{48}Ca, their last shell is unoccupied, and the excitation energy becomes again higher than for ^{48}Ca. We can observe the same tendency in Fig. 1(a) for the ^{X}Ar + ^{248}Cm reactions, in which the nucleus ^{46}Ar with magic neutron number obtains smaller excitation energy than the others. The ratio $R^{P/T}$ for the ^{40}Ca+ ^{248}Cm and ^{48}Ca+^{248}Cm reactions is practically the same [Fig. 2(a)]. For the ^{40,48}Ca+^{238}U [Fig. 3(a)] we have obtained different results on account of the effects of shell structure peculiarities of the target nucleus. We can conclude that the shell structure of nuclei (magic numbers, level densities near the Fermi surfaces of nuclei) as well as proton energy separation in the projectile (that is strongly connected with the N/Z ratio) and the relative position of Fermi surfaces of the interacting nuclei are important in distributions of the excitation energy and nucleons between the binary products of deep inelastic heavy ion collisions.

It is seen (Figs. 1, 2, 3, 7) that in all these reactions an increase in the orbital angular momentum (decrease in the total excitation energy) leads to an increase in the $R^{P/T}$ and $R^{\rm ph/ex}$ ratios. This means that the relative contribution of

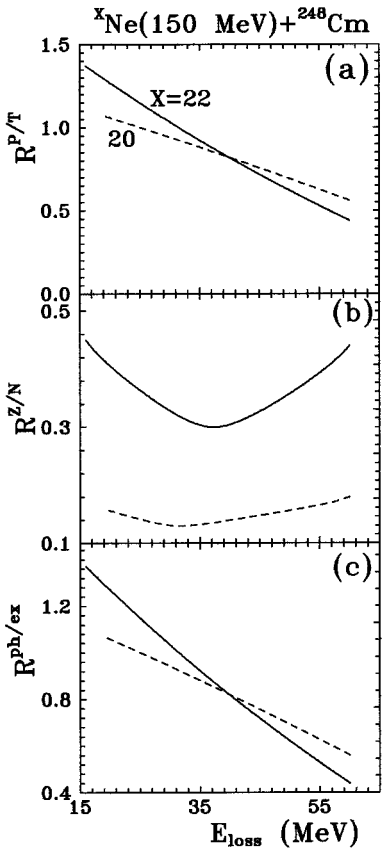

FIG. 7. The same as in Fig. 1, but for the ^{X}Ne+^{248}Cm reactions: $X=20$ (dashed line), $X=22$ (solid line).

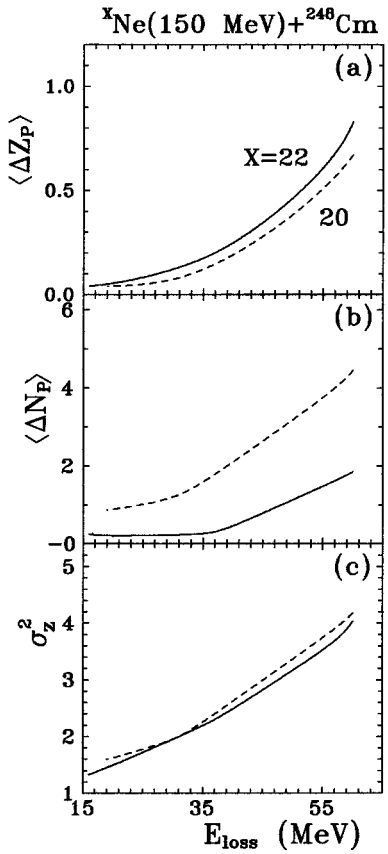

FIG. 8. The same as in Fig. 4, but for the ^{X}Ne+^{248}Cm reactions: $X=20$ (dashed line), $X=22$ (solid line).

particle-hole excitations to the total excitation energy of the dinuclear system also increases with the initial orbital angular momentum. It is clear that when the relative distance between the interacting nuclei increases (i.e., overlapping of the nuclear densities decreases), the probability of nucleon exchange decreases more rapidly than that of the inelastic excitations of nuclei.

The results of the $R^{\mathrm{ph/ex}}$ and $R^{Z/N}$ ratio calculations (see Figs. 1, 2, 3, and 7) are sensitive to the value of the N/Z ratio of the projectile nucleus. From the values of the $R^{\mathrm{ph/ex}}$ ratio one can conclude that nucleon exchange is the main mechanism of kinetic energy dissipation. Comparison of the values of $R^{\mathrm{ph/ex}}$ and $R^{Z/N}$ shows that with increasing projectile mass number, the contribution of the proton subsystem to the total excitation energy increases and becomes comparable to that of neutron exchange [Figs. 1(b), 2(b), 3(b), and 7(b)]. This enhancement of the role of the proton subsystem in the dissipation process with the increasing projectile N/Z ratio is attributed to the increase in the proton separation energy. As a result, the intensity and direction of the proton (neutron) transfer [Figs. 4(a), 4(b), 5(a), 5(b), 6(a), 6(b), 8(a), and 8(b)] between the fragments of the dinuclear system are changed.

The increase in the separation energy means that the proton Fermi level in the projectile with the larger N/Z ratio is deeper than in a projectile with a smaller N/Z. A large difference between the Fermi levels of interacting fragments can increase the number of transferred protons from the target to the projectile. Application of a heavy isotope as a projectile increases the difference between the last filled proton level of the projectile nucleus and first unfilled level of the target nucleus. As a result, the average excitation energy per proton transfer between a heavier projectile isotope and the target nucleus will be larger than that between a lighter projectile and the same target. This effect appears as an increase in the mean energy of the proton subsystem displayed in the increase in $R^{Z/N}$ [Figs. 1(b), 2(b), 3(b), 7(b)] and $R^{\mathrm{ph/ex}}$ [Figs. 1(c), 2(c), 3(c), 7(c)] ratios. The contribution of

TABLE I. The proton (S_p) and neutron (S_n) separation energies of Ne, Ar, Ca, $S_p=-7.62$ (^{238}U), -7.13 (^{248}Cm); $S_n=-6.15$ (^{238}U), -6.21 (^{248}Cm) [52].

Element	Ne		Ar			Ca			
A	20	22	34	40	46	40	44	48	54
S_p (MeV)	−12.85	−15.27	−4.67	−12.53	−18.51	−8.33	−12.17	−15.81	−22.00
S_n (MeV)	−16.87	−10.36	−17.07	−9.87	−7.22	−15.64	−11.13	−9.94	−5.51

the proton particle-hole excitation energy in the nuclei to the shared total excitation energy will be significant at large values of the orbital angular momentum. As follows from our results, the sharing of the total excitation energy between reaction partners and the distribution of the shared excitation energy between the proton and neutron subsystems of the nucleus should be correctly taken into account in calculating the preequilibrium nucleon yields.

In Figs. 4(a), 4(b), 5(a), 5(b), 6(a), 6(b), 8(a), and 8(b) the changes of the mean value of proton ($\langle \Delta Z_P \rangle$) and neutron ($\langle \Delta N_P \rangle$) numbers in projectilelike fragments of the ^{40,48}Ca + ^{238}U, ^{34,40,46}Ar + ^{248}Cm, ^{40,44,48,54}Ca + ^{248}Cm, and ^{20,22}Ne + ^{248}Cm reactions, as functions of $E_{\rm loss}$, are presented. The change in the $\langle \Delta Z_P \rangle$ and $\langle \Delta N_P \rangle$ decreases with $E_{\rm loss}$ because of a reduction in the overlap of nuclei. From Table I and Figs. 4(a), 4(b), 5(a), 5(b), 6(a), 6(b), 8(a), and 8(b) the sensitivity of $\langle \Delta Z_P \rangle$ and $\langle \Delta N_P \rangle$ to the proton and neutron separation energies is seen. In Figs. 4(a), 4(b), our results are compared with the experimental data for $\langle \Delta Z_P \rangle$ and $\langle \Delta N_P \rangle$ for secondary products of the ^{40,48}Ca+ ^{238}U reactions from [17]. Our results correspond to the primary products. According to our calculations, in the ^{40,44}Ca+ ^{248}Cm reactions, the centroid of the charge distribution moves to increase the charge asymmetry, in agreement with the experimentally observed increase in the yields of nuclides with masses greater than the mass of the target nucleus [18,20]. In the reaction with ^{48}Ca, the charge distribution centroid is shifted to decrease the charge asymmetry, which also agrees with the increase in the experimentally observed [18,20] yields of nuclides with masses smaller than the mass of the target nucleus. Unfortunately, for some characteristics of the reactions the experimental data are not complete.

IV. CONCLUSION

These theoretical results show that the shell structure and the N/Z ratio of the projectile strongly affect the excitation energy sharing between fragments and the mass (charge) distribution of reaction products in deep inelastic heavy ion collisions. For strongly asymmetric combinations, such as ^{20,22}Ne+ ^{248}Cm, ^{34,40,46}Ar+ ^{248}Cm, ^{40,48}Ca+ ^{238}U, and ^{40,44,48,54}Ca+ ^{248}Cm, the excitation energy is about equally shared between the products of the binary reactions. It should be noted that in all these reactions the ratio of the excitation energy of the projectilelike nucleus to that of the targetlike nucleus decreases with the initial orbital angular momentum. The contribution of the proton exchange to the total excitation energy increases with the neutron number in the projectile nucleus and becomes comparable to the contribution from the neutron exchange. The nucleon exchange between interacting fragments is the main mechanism of the relative motion kinetic energy dissipation. The relative contribution of particle-hole excitations (mainly protons) to the excitation energy of nuclei also increases with the initial orbital angular momentum.

Our calculations show that the excitation energy of heavy products of the reactions should not be large. Therefore, the probability of particle evaporation from heavy fragments should be small. The authors of the experimental work of [18,20] came to the same conclusion on the basis of the narrow form of isotope distributions. For practical purposes, knowledge about the excitation energy distribution between fragments can be used to reconstruct primary reaction product yields [23]. The results demonstrate the sensitivity of excitation energy sharing to the N/Z ratio; they are important enough to deserve detailed comparisons with experiments. We point out proton energy separation, in neutron-rich (heavy) projectiles, as the leading parameter, which is not inconsistent with former studies.

ACKNOWLEDGMENTS

We are grateful to Dr. N. V. Antonenko for fruitful discussions which stimulated the writing of this paper. We wish to thank Dr. F. Akilov, Dr. Zh. Kurmanov, and Ann Schaeffer for their effort in preparing this manuscript. G.G.A., R.V.J., and N.A.K. are grateful to the International Science Foundation for financial support under Grant No. RFJ-000 and the Russian Foundation of Fundamental Research (Grant No. 95-02-05684).

[1] V.V. Volkov, Phys. Rep. **44**, 93 (1978).
[2] W.U. Schröder and J.R. Huizenga, in *Treatise on Heavy-Ion Science*, edited by D.A. Bromley (Plenum, New York, 1984), Vol. 2, p. 115.
[3] J. Toke and W.U. Schröder, Annu. Rev. Nucl. Part. **42**, 401 (1992).
[4] R. Vandenbosh, A. Lazzarini, D. Leach, D.-K. Lock, A. Ray, and A. Seamster, Phys. Rev. Lett. **52**, 1964 (1984).
[5] T.C. Awes, R.L. Ferguson, R. Novotny, F.E. Obenshain, F. Plasil, S. Pontoppidan, V. Rauch, G.R. Young, and H. Sann, Phys. Rev. Lett. **52**, 251 (1984).
[6] D.R. Benton, H. Breuer, F. Khazaie, K. Kwiatkowski, V. Viola, S. Bradley, A.C. Mignerey, and A.P. Weston-Dawkes, Phys. Rev. C **38**, 1207 (1988).
[7] J. Toke, W.U. Schröder, and J.R. Huizenga, Phys. Rev. C **40**, R1577 (1989).
[8] D. Pade, W.U. Schröder, J. Toke, J.L. Wile, and R.T. de Souza, Phys. Rev. C **43**, 1288 (1991).
[9] R. Planeta, K. Kwiatkowski, S.H. Zhou, V.E. Viola, H. Breuer, M.A. McMahan, J. Randrup, and A.C. Mignerey, Phys. Rev. C **39**, R1197 (1989).
[10] R. Planeta, K. Kwiatkowski, S.H. Zhou, V.E. Viola, H. Breuer, M.A. McMahan, W. Kehoe, and A.C. Mignerey, Phys. Rev. C **41**, 942 (1990).
[11] K. Kwiatkowski, R. Planeta, S.H. Zhou, V.E. Viola, H. Breuer, M.A. McMahan, and A.C. Mignerey, Phys. Rev. C **41**, 958 (1990).
[12] J. Toke, R. Planeta, W.U. Schröder, and J.R. Huizenga, Phys. Rev. C **44**, 390 (1991).
[13] H. Keller, B. Bellwied, K. Lützenkirchen, J.V. Kratz, W. Brüchle, H. Gäggler, K.J. Moody, M. Schädel, and G. Wirth, Z. Phys. A **328**, 255 (1987).

[14] G. Beier, J. Friese, W. Henning, P. Kienle, H.J. Körner, W. Wagner, W.A. Mayer, and W. Mayer, Z. Phys. A **336**, 217 (1990).
[15] T. Tanabe, R. Bock, M. Dakowski, A. Gobbi, H. Sann, H. Stelzer, U. Lynen, A. Olmi, and D. Pelte, Nucl. Phys. **A342**, 194 (1980).
[16] K.D. Hildenbrand, H. Freiesleben, F. Pühlhofer, W.F.W. Schneider, R. Bock, D.V. Harrach, and H.J. Specht, Phys. Rev. Lett. **39**, 1065 (1977); Z. Phys. A **292**, 171 (1979).
[17] R.T. de Souza, W.U. Schröder, J.R. Huizenga, J. Toke, J.L. Wile, and S.S. Datta, Phys. Rev. C **39**, 114 (1989).
[18] D.C. Hoffman, M.M. Fowler, W.R. Daniels, H.R. von Gunten, D. Lee, K.J. Moody, K.E. Gregorich, R. Welch, G.T. Seaborg, W. Brüchle, M. Brügger, H. Gäggeler, M. Schädel, K. Summerer, G. Wirth, Th. Blaich, G. Herrman, N. Hildenbrand, J.V. Kratz, M. Lerch, and N. Trautmann, Phys. Rev. C **31**, 1763 (1986).
[19] R.T. de Souza, J.R. Huizenga, and W.V. Schröder, Phys. Rev. C **37**, 1901 (1988).
[20] A. Türler, H.R. von Gunten, J.D. Leuba, D.C. Hoffman, D.M. Lee, K.E. Gregorich, D.A. Bennet, R.M. Chasteler, C.M. Gannett, H.L. Hall, R.A. Henderson, and M.J. Nurmia, Phys. Rev. C **46**, 1364 (1992).
[21] J.L. Wile, S.S. Datta, W.U. Schröder, J. Tõke, D. Pade, S.P. Baldwin, J.R. Huizenga, B.M. Quednau, R.T. de Souza, and B.M. Szabo, Phys. Rev. C **47**, 2135 (1993).
[22] C.H. Dasso, G. Pollarolo, and A. Winther, Phys. Rev. Lett. **73**, 1907 (1994).
[23] N.V. Antonenko, E.A. Cherepanov, A.S. Iljinov, and M.V. Mebel, J. Alloys Compounds **213/214**, 460 (1994).
[24] H. Hofmann and P.J. Siemens, Nucl. Phys. **A257**, 165 (1976); **A275**, 464 (1977).
[25] G. Bertsch and R. Schaeffer, Nucl. Phys. **A277**, 509 (1977).
[26] D.H.E. Gross and H. Kalinowski, Phys. Rep. **45**, 175 (1978).
[27] K. Sato, S. Yamaji, K. Harada, and S. Yoshida, Z. Phys. A **290**, 149 (1979).
[28] P.J. Johansen, P.J. Siemens, A.S. Jensen, and H. Hofmann, Nucl. Phys. **A288**, 152 (1977).
[29] J. Randrup, Nucl. Phys. **A307**, 319 (1978); **A327**, 490 (1979); **A383**, 468 (1982).
[30] S. Ayik, Z. Phys. A **292**, 257 (1979).
[31] D. Agassi, C.M. Ko, and H.A. Weidenmüller, Ann. Phys. (N.Y.) **117**, 407 (1979).
[32] J. Bartel and H. Feldmeier, Z. Phys. A **297**, 333 (1980).
[33] S. Pal and N.K. Ganguly, Nucl. Phys. **A370**, 175 (1981).
[34] S. Ayik and W. Nörenberg, Z. Phys. A **309**, 121 (1982).
[35] S. Yamaji and A. Iwamoto, Z. Phys. A **313**, 161 (1983).
[36] H.J. Krappe, Nucl. Phys. **A505**, 417 (1989); **A505**, 139 (1986).
[37] F. Catara and E.G. Lanza, Nucl. Phys. **A451**, 299 (1986).
[38] M. Baldo, A. Rapisarda, R.A. Broglia, and A. Winther, Nucl. Phys. **A472**, 333 (1987).
[39] Z. He, P. Rozmej, and W. Nörenberg, Nucl. Phys. **A473**, 342 (1987).
[40] H. Feldmeier, Rep. Prog. Phys. **50**, 1 (1987).
[41] R.V. Jolos, R. Schmidt, and J. Teichert, Nucl. Phys. **A249**, 139 (1984).
[42] J. Blocki, Y. Boneh, J.R. Nix, J. Randrup, M. Robel, A.J. Sierk, and W.J. Swiatecki, Ann. Phys. (N.Y.) **113**, 330 (1978).
[43] G.G. Adamian, R.V. Jolos, and A.K. Nasirov, Z. Phys. A **347**, 203 (1994).
[44] G.G. Adamian, N.V. Antonenko, R.V. Jolos, and A.K. Nasirov, Phys. Part. Nucl. A **25**, 583 (1994).
[45] V.V. Volkov, No. D7-87-68 Dubna, 1987, p. 528 (International School-Seminar on Heavy Ion Physics, Dubna, 1986); in Proceedings of the 6th International Conference on Nuclear Reactions Mechanisms, Varenna, edited by E. Gadioli, 1991, p. 39.
[46] N.V. Antonenko and R.V. Jolos, Z. Phys. A **338**, 423 (1991).
[47] G.G. Adamian, R.V. Jolos, and A.K. Nasirov, Sov. J. Nucl. Phys. **55**, 660 (1992).
[48] G.G. Adamian, N.V. Antonenko, R.V. Jolos, and A.K. Nasirov, Nucl. Phys. **A551**, 321 (1993).
[49] H.S. Köhler, Nucl. Phys. **A343**, 315 (1980); **A378**, 181 (1982).
[50] D. Pines and P. Noziéres, *The Theory of Quantum Liquids* (Benjamin, New York, 1966).
[51] A.B. Migdal, *Theory of the Finite Fermi-System and Property of the Atomic Nucleus* (Moscow, Nauka, 1983).
[52] A.M. Wapstra and G. Audi, Nucl. Phys. **A565**, 1 (1993).
[53] R. Schmidt, G. Wolschin, and V.D. Toneev, Nucl. Phys. **A311**, 247 (1978).
[54] R. Schmidt, Part. Nucl. **13**, 1203 (1982).